HHS Public Access

Author manuscript

J Neural Eng. Author manuscript; available in PMC 2020 September 16.

Published in final edited form as:

J Neural Eng. 2018 June ; 15(3): 036018. doi:10.1088/1741-2552/aaa039.

Chronic cuffing of cervical vagus nerve inhibits efferent fiber integrity in rat model

Jesse P Somann[1,2], **Gabriel O Albors**[2,3], **Kaitlyn V Neihouser**[2,3], **Kun-Han Lu**[4], **Zhongming Liu**[1,3,4], **Matthew P Ward**[3,5], **Abigail Durkes**[6], **J Paul Robinson**[7], **Terry L Powley**[8], **Pedro P Irazoqui**[1,2,3]

[1]Department of Electrical and Computer Engineering, Purdue University, West Lafayette, Indiana, United States of America

[2]Center for Implantable Devices (CID), Purdue University, West Lafayette, Indiana, United States of America

[3]Weldon School of Biomedical Engineering, Purdue University, West Lafayette, Indiana, United States of America

[4]Purdue Laboratory of Integrated Brain Imaging, Purdue University, West Lafayette, Indiana, United States of America

[5]Indiana University School of Medicine, Indianapolis, IN, United States of America

[6]Department of Comparative Pathobiology, Purdue University, West Lafayette, Indiana, United States of America

[7]Purdue Cytometry Laboratories, Purdue University, West Lafayette, Indiana, United States of America

[8]Department of Psychological Sciences, Purdue University, West Lafayette, Indiana, United States of America

Abstract

Objective—Numerous studies of vagal nerve stimulation (VNS) have been published showing it to be a potential treatment for chronic inflammation and other related diseases and disorders. Studies in recent years have shown that electrical stimulation of the vagal efferent fibers can artificially modulate cytokine levels and reduce systematic inflammation. Most VNS research in the treatment of inflammation have been acute studies on rodent subjects. Our study tested VNS on freely moving animals by stimulating and recording from the cervical vagus with nerve cuff electrodes over an extended period of time.

Approach—We used methods of electrical stimulation, retrograde tracing (using Fluorogold) and post necropsy histological analysis of nerve tissue, flow cytometry to measure plasma cytokine levels, and MRI scanning of gastric emptying. This novel combination of methods allowed examination of physiological aspects of VNS previously unexplored.

jsomann@purdue.edu.

Supplementary material for this article is available online

Main results—Through our study of 53 rat subjects, we found that chronically cuffing the left cervical vagus nerve suppressed efferent Fluorogold transport in 43 of 44 animals (36 showed complete suppression). Measured cytokine levels and gastric emptying rates concurrently showed nominal differences between chronically cuffed rats and those tested with similar acute methods. Meanwhile, results of electrophysiological and histological tests of the cuffed nerves revealed them to be otherwise healthy, consistent with previous literature.

Significance—We hypothesize that due to these unforeseen and unexplored physiological consequences of the chronically cuffed vagus nerve in a rat, that inflammatory modulation and other vagal effects by VNS may become unreliable in chronic studies. Given our findings, we submit that it would benefit the VNS community to re-examine methods used in previous literature to verify the efficacy of the rat model for chronic VNS studies.

Keywords

vagus nerve stimulation; inflammation; chronic implantation; fluorogold; flow cytometry; cuff electrode; gastric emptying

1. Introduction

1.1. Background and hypothesis

Vagal nerve stimulation (VNS) therapy has become a prominent fixture in treatment research and has been proposed as a therapy for ailments such as depression [1], rheumatoid arthritis [2], obesity [3], and many others. While the FDA has approved VNS for seizure prevention in epilepsy and as an alternative for drug-resistant depression [4, 5], the exact mechanics of much of the body's response to VNS has yet to be characterized. One such area is VNS for the modulation of inflammation in the gastrointestinal (GI) tract. It was hypothesized by Tracey in 2002 [6] that vagal efferent fibers to the spleen modulated cytokine release through an 'inflammatory reflex' that could produce a therapeutic anti-inflammatory effect. Since then there has been ample research conducted to explore and dispute details of this inflammatory reflex [7–11], but much of the specific mechanisms for cytokine modulation remain undefined.

There are two major aspects to consider when studying effects of VNS. The first is that the cervical vagus is populated with both sensory afferent fibers (~80%) and efferent motor fibers (~20%). Afferent fibers collect in the nodose ganglia of the vagus nerve before reaching to the nucleus of the solitary tract (NTS) in the medulla oblongata, while efferent motor fibers originate from the dorsal motor nucleus (DMN) of the medulla. These fibers serve many separate and distinct functions of the nervous system but are also connected within a parasympathetic system that contributes to the inflammatory reflex [12] and could cause possible conflicting effects between the two fiber types with VNS. Some studies have circumvented this potential offset by chemically or electrically attenuating the functionality of a specific fiber type [13–15].

The second major aspect to consider is whether to attempt a chronic or acute study. There are ample acute studies that have been performed on the topic of anti-inflammatory pathways using rodent models [8, 13, 16–18]. Nonrecovery studies give researchers the

ability to evaluate the physiological effects of rats in a controlled environment, allowing idealized set-ups for surgical processes, precise stimulation electrode placement with reduced noise (due to shorter electrical leads), and easier use of faradaic cages. Long term effects of treatment over days, weeks, and even years cannot be accurately studied acutely. Also, due to the nature of the anesthetic used in acute surgical procedures, potential unintended and detrimental physiological effects on the body's normal state can be caused [19]. As was explored by Picq *et al* [20], the immunoregulatory effects of isoflurane can influence the results of studies aimed at anti-inflammatory effects of VNS.

We resolve that the best option for studying the true effects of VNS for the treatment of inflammation and many other physiological effects remains a reliable long-term chronic study on an awake and freely moving subject. Our exper imental design was a chronic study identifying effects of left cervical VNS on inflammation in the GI tract of rats.

In this study, we utilized novel combinations of verification techniques on 53 rats to analyze multiple dynamic effects of VNS on the physiology of the nerve. These included retrograde tracer analysis using fluorogold (FG), electrophysiological responses to stimulation, visual and histological analyses of nerve samples, and plasma analysis of cytokine levels (animal names and results can be found in supplemental table 1 (stacks.iop.org/JNE/15/036018/mmedia)). As a result, we discovered complete suppression of FG transport to the DMN of the medulla in animals that had vagus nerves cuffed for periods ranging from 13 to 71 d in length, and found insignificant modulation of inflammatory cytokines when applying VNS therapy, as compared to corresponding acute subjects. In addition, we performed gastric emptying tests using magnetic resonance imaging (MRI) on six chronically implanted rats (details in supplemental table 2) to compare with equivalent acute testing in a parallel study. Results revealed attenuated effects on gastric emptying rates when the vagus nerve was chronically cuffed.

Our resulting hypothesis, that the rat model may be unsuited for chronic nerve stimulation studies, is compelling and pertinent to the entire VNS community. We revealed evident flaws related to chronic cuffing of the vagus nerve in a rat model, as it creates previously unstudied physiological effects that suppress the FG transport mechanism, and ostensibly, act to suppress the anti-inflammatory and other effects of VNS. This hypothesis stands despite the outward appearance and functionality of a healthy nerve using traditional methods of integrity verification (visual, histological, electrophysiological).

Given the scarcity of related literature to verify or disprove our findings, we feel that while our results do not invalidate the findings of past chronic studies in rats due to differences in methods used, they do call into question the integrity of facets of some data. If indeed some undetected aspect of the efferent (and possibly afferent) fiber physiological operation was affected by cuffing of the peripheral nerve, then the resulting biological effects of the subject matter could also have been attenuated or completely altered by the compromised nerve fibers.

1.2. Comparative review of chronic cuff VNS studies in rats

A comparative literature review of 17 recent studies (details in supplemental tables 3 and 4) employing chronic methods of VNS varied widely in application but revealed few common methods to contrast our experiment.

Most of the chronic VNS studies reviewed centered on biological effects related primarily to brain activity, such as seizures (epilepsy), depression, and memory, and primarily due to stimulation of afferent fibers of the vagus nerve [15, 21–28]. While there are likely secondary and indirect effects to the overall autonomic peripheral nervous system response due to efferent fiber activation from VNS, evidence suggests that VNS affects the brain primarily through afferent fiber activation and not through indirect efferent effects [4]. Studies that focused on primarily efferent targets of VNS were rare, with four groups specifically studying cardiac effects [29–32]. Only Meregnani *et al* [33] centered on the topic of inflammation in the gastric region of the body as we sought to.

None of the reviewed literature implemented our retrograde tracer (FG) analysis into their studies of chronic nerve stimulation. We argue this to be a definitive and critical evaluative measure of nerve functionality. To our knowledge, we are the first to use it in a VNS study.

Merely two of the reviewed papers included a mechanism to directly record compound nerve action potentials (CNAPs) from the nerve [14, 34]. Other groups relied instead on physiological indicators such as changes in measured heart rate [28–30] to verify that VNS was operating as intended or having an effect.

While histological analysis is common in developmental studies of new cuff designs [35–37], none of the reviewed studies published a histological analysis of the effect of their cuffs on the nerve during implantation. With such a depend ence on the cuff/nerve interface for VNS studies and the multiple variables involved in a chronic cuff implantation including materials used, surgical techniques, and animal variances just to name a few, we felt this was a necessary analysis to include.

Three groups performed histochemical analyses of inflammatory cytokines. Chunchai *et al* [25] measured tumor necrosis factor alpha (TNF-α) levels in brain and plasma samples, while Chapleau *et al* [30] measured multiple cytokines in serum only and Meregnani *et al* [33] measured various cytokine levels directly from colon tissue samples. In comparison, we tested blood (plasma) samples on 13 different cytokine variants.

2. Methods

2.1. Experimental timing

The order and timing of multiple procedures involved in this chronic study are outlined in figure 1. All parts of this experiment were organized and run to minimize unplanned variations to timing and techniques.

2.2. Materials

2.2.1. Nerve cuffs—Our standard cuff electrodes were custom made from 1 × 7 × 0.001″ (75 μm OD) braided Platinum Iridium (Pt/Ir) wire (Fort Wayne Metals; Fort Wayne, IN) threaded into a medical grade silicone tubing substrate (0.03″ ID; A-M Systems; Carlsborg, WA). A single strand of the wire was threaded through the inside of the cuff, following its contour, to create an electrode that would surround over 70% of the nerve diameter when implanted. The cranial electrode of the stimulation cuff required a larger exposed surface area due to its use as the grounding place for our system's device electronics. To accomplish this, we threaded the Pt/Ir wire around the inner and outer contours of the cuff six times (shown in supplemental figure 1) effectively increasing the electrode surface area by 15×. The lead tubing was fastened and sealed to the cuff with a fast curing silicone adhesive (Med2–4213; NuSil; Carpinteria, CA). The cuffs were 3 mm in length with Pt/Ir electrodes spaced approximately 1 mm apart.

In addition to our standard cuff design, we attempted to use three other electrode varieties:

- CorTec tunnel cuff with PtIr electrodes. Cuff was 3 mm in length with a 0.6 mm inner diameter. Stimulation cuff only was implanted on animal eRx118. (Cat. No. 1041.2008.01; CorTec; Freiburg, Germany)
- Shape memory polymer cuff fabricated by University of Texas—Dallas as presented in figure 2(g) of Ware *et al* [38]. Our variant had only two electrode traces and only the stimulation cuff was implanted on animal eRx111.
- Experimental thin film cuffs using two gold traces and pads on a 12 μm thick parylene substrate. The 4.7 mm long and 2.3 mm wide cuff electrodes were gently wrapped around the isolated vagus nerve to create ~1.5 mm diameter cuffs with separate 11 mm tables wrapped around the cuffed nerve and carotid artery for anchoring. Excess table material was cut away and Kwik-Sil was used to fasten the interface in place. Record and stimulation cuffs were implanted on eRx119. The authors can be contacted for more details on this cuff design.

2.2.2. Devices/headcaps—The stimulation and recording for most of our chronic rat tests were done using the Bionode; a multipurpose implantable platform designed for physiological studies [39]. For this study, the Bionode was typically implemented with a single stimulation and a single record channel, each with a cuff electrode attached. The Bionode can produce bi-phasic constant current stimulation profiles ranging from 50 μA to 1.1 mA in amplitude and 50 μs to 1 ms in pulse width through the stimulation cuff electrodes. The recording electrodes get fed through a dual stage differential amplifier. The Bionode's interface allowed real-time recording and control of stimulations to the implanted device, using a custom software platform.

Instead of using a fully implanted Bionode, we tested some of our animals with a tethered setup using a cranial headcap. This was done to vary the surgical method of some animals and verify our findings. For these animals, the headcaps were pre-built by attaching our nerve cuffs to individual pins (PlasticsOne; Roanoke, VA) and affixing those pins to headcap

pedestals (Plastics One) with dental cement. We also used headcaps with single implanted stimulation cuffs for chronic gastric emptying experiments.

2.3. Surgical methods

2.3.1. General animal preparation—All surgical methods and animal handling are approved by the Institutional Animal Care and Use Committee (IACUC). Male Sprague Dawley rats weighing between 175–199 g were used for data collection and housed under standard conditions. Prior to surgery, animals were given ad-libitum access to food and water. A pre-operative analgesic, butorphanol (0.5–2 mg kg^{-1}, SC) or buprenorphine (0.05–0.1 mg kg^{-1}, SC), were administered immediately prior to surgery and 4–6 doses thereafter for 48 h post-operative. All surgical equipment was sterilized and the animals underwent standard aseptic surgical preparation. Immediately following induction of anesthesia (isoflurane, oxygen delivered at 0.5 to 1.0 l min^{-1}, 1 to 4%), the surgical site was shaved and scrubbed with Betadine and sterile alcohol pads.

Acute surgery followed similar general surgical procedures, but a ketamine/xylazine cocktail with a 75 mg kg^{-1} ketamine and 5 mg kg^{-1} xylazine ratio was used as an alternative anesthetic to ensure proper nerve function. The dosage was determined by weight. We note that due to perceived limits to the effectiveness of this anesthetic for long periods of time, that only 90 min of blood collections (post lipopolysaccharide (LPS) challenge) were collected versus the 120 min done with the chronic animals.

2.3.2. Device implantation—With the rat in the prone position, we made incisions on the side or back of the rat to facilitate the placement of the implantable device. A subcutaneous pocket was created and the device inserted into the pocket, oriented, and then sutured in place. After moving the rat to the lateral recumbent position, we created a midline incision on the neck and routed the electrodes subcutaneously to the neck. Incisions made to implant the device were next sutured closed. With the rat in the supine position we expanded the midline incision to start at the jaw line moving caudally. We reflected the skin and soft tissue to expose the underlying sternohyoid and sternocleidomastoid muscles, which sit atop the carotid sheath. Surgical retractors were carefully placed to hold open the incision site. Using a blunt dissection technique, we gently separated the soft and connective tissues until the trachea and carotid artery sheath could be seen. The cervical vagus nerve sits adjacent and runs parallel to the carotid artery above the level of the carotid bifurcation. We carefully dissected the connective tissues surrounding the vagus nerve exposing the nerve. One or two cuff electrodes were then wrapped around the exposed vagus nerve (if two, stimulation cuff rostral and recording cuff caudal to the omohyoid muscle) and cuffs were secured shut with a suture or Kwik-Sil Silicone Elastomer (World Precision Instruments, Inc.; Sarasota, FL), and any extra lead was curved into a strain relief loop and sutured to neighboring muscle tissue or skin to minimize movement of the cuff electrode. We then sutured the incision closed. During tethered procedures, no device was not implanted and electrodes were terminated into a headcap and cemented to the skull. In some cases, we routed additional leads subcutaneously from the device to a transdermal connector port behind the shoulder blades to guarantee power fidelity while collecting blood.

Similar surgical procedures were followed for acute LPS experiments with stimulation and recording cuffs being placed around the cervical vagus nerve and then attached to an externally placed Bionode for the duration of the experiment.

2.4. FG injection

Analysis of retrograde tracer transport of the vagal efferent fibers to the DMN has been shown to be an effective means of verifying selective vagotomies of the five subdiaphragmatic vagal branches in the GI tract. Each of the five branches has been shown to transport to distinct areas of the DMN, with the left vagal branches (hepatic, accessory celiac, and ventral gastric) accumulating in the left side of the DMN and the right branches (dorsal celiac and dorsal gastric) to the right side of the DMN [40]. We used established methods of FG administration to verify the physiological efficacy of the left and right vagal efferent fibers [40–42].

Approximately 5 d prior to blood collection, stimulation, and perfusion, we gave animals an intraperitoneal injection of 1 mg/1 ml saline of FG (Fluorochrome, Inc.; Englewood, CO) that labels cell bodies of intact efferent fibers in the DMN.

2.5. Catheter placement and blood collection

Blood samples were obtained to track circulating levels of inflammatory cytokines. We followed procedures outlined in the NIH Guidelines for Survival Bleeding of Mice and Rats for blood sampling. The amount of blood collected did not exceed the maximum allowed 10% of the circulating blood volume. We surgically placed catheters in the rats ~24 h prior to blood collection following femoral cannulation procedures outlined in the Bioanalytical Systems, Inc. Culex surgical manual [43] and then placed the rats into the Culex Automated *in vivo* Sampling System (Bioanalytical Systems Inc.; West Lafayette, IN) [44] while connected to the Raturn caging system (Bioanalytical Systems Inc.) [45]. We programmed the Culex system to automatically collect ~200 μl blood samples from each rat at predefined intervals of 30 min over a 3 h timeframe as outlined in figure 2.

The Culex was not used for acute LPS experiments. Instead, blood was obtained by punctured leg vessels, and samples collected into K3 ETDA coated minivette tubes. Only four blood collections were taken for acute animals at times of − 30, 30, 60, and 90 min with respect to LPS injections.

2.6. Testing procedures

2.6.1. LPS preparation/injection—LPS solution was prepared immediately prior to blood collections in the animals in a dose of 5 mg kg^{-1}. We measured LPS (Sigma-Aldrich, serotype O111:B4) into 1.5 ml Eppendorf tubes using a Mettler Toledo AB54-S/FACT digital scale and added sterile saline (0.9% sodium chloride) to the tube in a proportion of 0.2 ml saline/1 mg LPS. The solution was sonicated for 30 + min prior to usage. We administered LPS intravenously (chronic) or intraperitoneally (acute) at the specified time during blood collection procedures, and before stimulation treatments if applicable.

2.6.2. Stimulation—We performed all stimulations with balanced, bi-phasic, square wave pulses produced by either our in-house implantable BioNode system that is described in previous work [39], or equivalently by a National Instruments USB-6343 Multifunction Device (NI-DAQ; National Instruments; Austin, TX) for select animals tethered with a headcap configuration. The recording channel consisted of a differ ential two-stage filter/amplifier. The first stage was a low power instrumentation amplifier (INA333; Texas Instrument; Dallas, TX) configured for a gain of 20 dB, and the second stage was an inverted operational amplifier (OPA313, Texas Instrument) configuration designed for a gain of 40 dB and bandwidth from ~15 Hz to ~3 kHz. The total record channel gain was 60 dB. The stimulation was produced by a common mode volt age difference amplifier (LT6375; Linear Technology; Milpitas, CA) configured to act as a Howland Current Pump, and controlled either by the on-chip microcontroller (nRF51822; Nordic Semiconductor; Trondheim, Norway) paired with a digital-to-analog converter (DAC7551, Texas Instrument) on the BioNode or the output of the NI-DAQ.

Our system has been shown to allow fully autonomous neural control (ANC) in rats by Ward *et al* [46] in acute test environments, and has been used in other recent studies [47]. In our acute experiments, we attempted ANC calibrations immediately after the first blood sample, and 30 min prior to LPS injection in the animal. During calibration, we used ANC to determine a maximal activation profile for a CNAP response (B or C fiber) to various stimulation profiles varied in amplitude and pulse duration. Due to the highly variable environments experienced in our chronic tests however, we did not utilize the fully autonomous functions for most of our chronic animals. Instead, we manually tested different stimulation profiles in real-time to determine an optimal profile to induce a CNAP response. If successful maximal nerve activation was detected, we ran stimulation for 5 min at 5 Hz at the corresponding stimulation profile. If not, we utilized a pre-determined and default maximal activation stimulation profile (1 mA amplitude, 1 millisecond pulse duration, 5 Hz) for the 5 min stimulation. We utilized a stimulation frequency of 5 Hz which is in the range of normal nerve traffic in the vagus nerve [48].

2.6.3. Perfusion and brain tissue preparation—After the final blood collections, animals were deeply anesthetized with a lethal dose of Ketamine/Xylazine followed by a transcardial perfusion with 300 ml of 0.9% saline at 40 °C, followed by 400 ml of 4% paraformaldehyde at 4 °C. We then removed the medulla and cryoprotected it overnight in 15% sucrose in 4% paraformaldehyde at 4 °C. Serial 40 μm coronal sections were taken with a cryostat between the level of the facial nucleus and the pyramids. We collected sections onto gelatin-coated microscope slides, dehydrated and cleared them in alcohol and xylene, and then placed the sections under a coverslip with DPX (Sigma-Aldrich, St. Louis, MO).

2.7. Sample processing and analysis

2.7.1. FG imaging (of medulla)—FG images of the medulla were acquired using a LEICA DMRE microscope with a SPOT FLEX camera controlled using SPOT Software (V5; Diagnostic Instruments, Sterling Heights, MI). We did final post-production using Photoshop CS6 (Adobe Systems, San Jose, CA). Photoshop was used to: (1) apply text and

scale bars; (2) make minor adjustments to the color, brightness, contrast, and sharpness of the images to match the appearance of the original material viewed under the microscope; and (3) to organize the final layout of the figures.

2.7.2. Necropsy nerve extraction and imaging—Most necropsy analysis was done post perfusion, making it difficult to locate specific nerve landmarks due to blending of tissue textures. Therefore, we visually evaluated some animals preperfusion to allow for improved observation and analysis.

We removed vagus nerve column (including carotid artery, superior cervical ganglia, and other surrounding tissues) samples to be analyzed for FG tracer from the animal using blunt dissection techniques, and placed them into a 4% paraformaldehyde solution.

Samples for imaging with a fluorescent microscope were dissected and positioned on clean glass slides to verify an optimal view. We then mounted them on gelatin coated (1.5% gelatin solution) Corning micro slides under a Leica M205 FA Stereomicroscope with a UV ET filter and illuminated them with a Prior Lumen 200 fluorescence illumination system. An uncoated Corning micro slide was placed on top of the nerve, and the nerve was crushed onto the gelatin coated slide by placing 4 lb weights on top of the slide for 1 h. We then removed the weights and the uncoated slide from the gelatin coated slide onto which the nerve had been crushed, and let the slide dry overnight. The slides were then dehydrated in a 2 min ascending series of alcohols (70% EtOH, 95% EtOH, 100% EtOH × 2) and xylene (6 min × 2), and then coverslipped with custom coverslips (Electron Microscopy Sciences).

Mosaic image *z*-stacks were collected with a Leica DFC310 FX camera connected to a Leica DM5500 microscope (D filter and HCS PL Fluotar 10 × /0.30 objective), using Surveyor software. We used the mosaic image stacks to create an all-infocus image using the Auto-Blend function in Photoshop CC.

2.7.3. Blood sample processing—For cytokine analysis, fresh blood was collected in EDTA (K3EDTA at 1.75 mg ml^{-1}), centrifuged at 2000 × g for 10 min, and plasma extracted and either prepared immediately or aliquoted and stored at − 20 °C. We analyzed plasma samples using a LEGENDplex™ Rat Th Cytokine Panel (13-plex) (Biolegend, San Diego, CA) in a V-bottom 96 well plate. This assay allowed simultaneous analysis of 13 cytokines, IL-2, IL-4, IL-5, IL-6, IL-9, IL-10, IL-13, IL-17A, IL-17F, IL-22, GM-CSF, IFN-γ and TNF-α, using a multiplexed fluorescent bead assay procedure as described. A sandwich based immunoassay was performed on 96 well plates using bead sets that had previously captured the analytes of interest. For each sample, we diluted plasma 4-fold with an assay buffer before testing it. Rat plasma samples were then distributed appropriately in duplicate on the plate and capture beads added to each well. Each analyte standard was added to a standard well, followed by serial dilutions. This established a standard curve for each plate. We incubated plates at room temperature for 2 h while shaking at 500 rpm. We then washed the plates twice by centrifugation. After washing, 25 μl of biotinylated detection antibody was added to each well and the plates were sealed and placed on a plate shaker (500 rpm) in the dark for 60 min. All wells then received 25 μl of the streptavidin with phycoerythrin (PE) and we resealed and incubated the plates at room temperature in the

dark on a plate shaker (500 rpm) for 30 min. Plates were washed again as previously, with addition of 200 μl wash buffer and centrifuged. 150 μl of wash buffer was then added to each well and beads resuspended by trituration. We then read the plates on the flow cytometer.

2.7.4. Flow cytometry—We read plates on one of two instruments: a CytoFlex 13 color cytometer (Beckman Coulter, Miami, Florida) or an Attune 14 color cytometer (Thermo Fisher, Eugene, Oregon). Allophycocyanin (APC) content was used to distinguish different capture beads. Setup for each instrument was similar and required calibration using instrument calibration beads to ensure the instruments were calibrated properly. The 96 well plates were automatically read by either flow cytometer and output files generated were standard FCS files. We set the instruments to collect 4000 beads per well, ensuring approximately 250–350 beads of each cytokine per well. Prior to running plates, we ran set-up beads included in the kit on each instrument to ensure the detection probe (PE) was properly calibrated and the bead probe (APC) was set at previously determined voltages to ensure the best bead separation.

2.7.5. Blood data extraction—Upon completion of each plate, FCS files were analyzed by MPLEX software (Doclu LLC, West Lafayette, In). The software opened the entire 96 listmode files, and upon identification of the bead signal (APC) and the detection signal (PE), it collected a two-parameter plot with APC on the *x*-axis and forward scatter on the *y*-axis. In this manner, the 13 populations of beads were resolved. For Legendplex bead assays, two bead sizes were discriminated by forward or side scatter and by bead intensity on the APC detection parameter. Each cytokine was then identified by its preset bead size and dye intensity level. There were six intensity levels for the smaller beads (A beads) and seven intensity levels for the larger (B beads). We identified the standard curves by their location on the 96 well plates and identified duplicates. The MPLEX software was preset for a Legendplex assay profile which associated either A beads or B beads with the appropriate cytokine. An automated clustering algorithm was used to fit the bead populations to the predesignated beads, and the standard curves for all 13 cytokines were automatically calculated, followed by production of a CSV output file with all well data.

2.7.6. Blood data analysis—Raw concentration signals from cytokines attached to functional beads were compared to calibration curves calculated for each plate of samples run, and used to produce cytokine concentration data for statistical analysis and figures. We averaged two replicates per sample before analysis.

Multivariate analysis of variance (MANOVA) was first performed on raw sets of all 13 measured cytokine concentrations collected from plasma samples. Post hoc analysis of variance (ANOVA) was also performed on raw sets of each cytokine concentration. To compensate for significant noise in the cytokine calibration curves (at low concentration levels), we converted raw data into fractions of the total cytokine signal for each sample. To then allow for Gaussian analysis to be performed, we computed angular arcsine transformations and corresponding Cohen's h effect sizes:

$$\phi = 2\arcsin\sqrt{p} \quad (1)$$

$$h = |\phi_1 - \phi_2| . \quad (2)$$

Where p is a given proportion and h is a resulting Cohen's h effect size. ANOVA analysis was again performed on the angular transformations. $P < 0.05$ was considered statistically significant, but we did note other scientifically significant trends that did not meet this threshold.

2.7.7. Histology—To further verify the integrity of the chronically implanted vagus nerve, cuffed nerve samples from eight rats were fixed and then embedded. We used paraffin molds for silicone cuffs with no metal electrode and poly-methyl methacrylate (PMMA) resin molds for cuffs with wire electrodes to prevent tearing of enclosed nerves. Specific details on these processes can be found in our supplemental materials.

2.8. Gastric MRI scanning

Surgical procedures for implanting stimulation cuffs in rats used for gastric emptying testing are in line with those outlined previously for headcaps, with the exception that we used only a single stimulation cuff and no recording cuff, and we limited headcaps to only two pins to reduce potential imaging artifact. All dietary training, scanning procedures, and image processing and analysis techniques mirrored those methods established by Lu *et al* [49].

Stimulation was performed using our Bionode system utilizing our standard cuffs as described earlier. We stimulated throughout the period of scanning, using balanced bi-phasic pulses of 600 μA, 360 μs, at 10 Hz. The parameters were determined by earlier collaborative testing to induce the largest EMG response on the stomach wall. Stimulation was applied continuously throughout the 4 h test period with trains of 20 s on followed by 40 s off. During stimulation scans, we noted that some rats showed severe signs of apnea and bradypnea resembling what was explored by Zaaimi *et al* [50]. These phenomena were commonly accompanied by a corresponding arrest in observed stomach motility during stimulation. It was not our goal here to explore this effect in detail, therefore, we excluded animals that exhibited this trait from our data.

3. Results

3.1. FG transport

Early in chronic VNS testing, we recognized an issue with efferent FG transport in the left (cuffed) vagus nerves of the animals. 36 of the 44 cuffed animals showed complete suppression of FG transport to the left side of the DMN in medulla samples, indicating a complete cervical vagotomy of the left vagal nerve, despite the animals receiving no surgical vagotomy. In addition, all animals demonstrated expected FG transport in the uncuffed right vagus nerve. Based on visual analysis during necropsy, it was first considered that the cause was likely due to surgical techniques, and mechanical stresses and migration of our cuff electrodes on the nerves.

A visual inspection of the left cervical vagus site was performed on 32 rats during necropsy. Early inspections revealed moderate to severe cuff migration and manipulation of the nerve

in several animals. We hypothesized that these issues were causing the lack of FG transport, prompting multiple iterations of surgical technique and materials improvements. Such included: added lead lengths and strain relief loops, increased flexibility of the lead materials, altered lead anchoring techniques and locations, changed wire electrode configurations within the cuffs (including inert cuffs with no metal electrode), implanted single stimulation cuffs (versus a second recording cuff as was standard for our study), employed multiple different surgeons, and tried multiple types of cuffs (as presented in our methods).

These changes produced significant visual decreases in mechanical strain to the nerve and all later subjects showed good integrity of cuffs and leads in the surgical site (shown in supplemental figure 2). Despite the adjustments and improved cuff/nerve interface integrity, FG transport results did not improve (figure 3). We, therefore, hypothesized that the cuffing of the nerve itself had a dominant effect on nerve physiology regardless of other external stresses.

To further explore the physiological phenomena, we extracted the right and left (still cuffed) vagus nerve columns from 18 rats during post perfusion necropsy. These nerve samples were observed under a fluorescence scope for signs of FG in the nerves and nodose ganglia and were then either mounted onto a slide to be photographed or fixed for basic H&E histology ($n = 8$). Samples that were extracted with both left and right nodose ganglia still intact ($n = 7$) were analyzed using a fluorescence microscope (details shown in supplemental figures 3 and 4). Observations showed that the ganglia of the cuffed left vagus nerves and the uncuffed right vagus nerves both contained FG illuminated cells, indicating an active FG transport in the afferent nerve fibers, despite a severe or complete suppression of efferent fibers to the medulla as demonstrated in figure 4 (additional images shown in supplemental figure 5).

It is important to note that FG brightness varied between animals as is common due to biological, surgical, and tissue extraction and processing variances. Despite this inconsistency, the trends noted above were present in all samples and there was no consistent difference observed in density of FG illumination between nodose samples from cuffed left vagus versus un-cuffed right vagus nerves.

3.2. CNAP detection

A complex, but telling, measure to test the integrity of a peripheral nerve during VNS is to record the responsive action potentials of the nerve to a prior electrical stimulation. CNAP recordings can provide a direct indication of the variety and extent of nerve fibers being activated by a given stimulation.

Recording CNAP responses in real time, however, is challenging due to multiple factors including noise in the stimulation or recording channels, and overlap of artifact in the signal due to the electrical stimulation and laryngeal [34, 51] and other muscle artifacts. This difficulty is compounded by factors related to the chronic test environment. As mentioned, most reviewed studies used pre-determined stimulation parameters and concentrated only on

analyzing the resulting biological data [28–30], or recorded the signal during testing and post-processed the data afterwards to determine the fiber response [14, 34].

In our study, we employed two nerve cuffs (one stimulation and one recording) that allowed simultaneous stimulation and recording in a closed-loop system [46]. Testing fiber responses resulting from stimulation is paramount due to frequent changes in the biology of an animal during recovery from implantation and due to foreign body response to the nerve cuffs. Literature has shown that impedances and the resulting nerve response to electrical stimulation can fluctuate for weeks and even months before stabilizing [52]. This was confirmed in our own testing by fluctuations in CNAP responses seen when tested on multiple days during recovery as seen in figure 5. It is important to note that stimulation parameters shown in figure 5 are significantly lower than those utilized during functional stimulation treatments. Functional stimulation in our LPS experiments utilized amplitudes of 1 mA or higher that were more likely to have recruited significant C-fiber activations.

For this animal we also saw larger potentials on day 36 (with rat freely moving) than on days 23 and 27 (rat anesthetized with isoflurane). Differences could be contributed in part to effects of being anesthetized and to peripheral stimulation effects such as laryngeal muscle and movement artifacts. Due to practical restraints such as limited surgical space near the vagus, we did not perform any formal testing for such artifacts in this study.

We did not endeavor here to make conclusions based on the labeled fiber types of CNAP responses presented in figure 5, but strictly to demonstrate that diverse CNAP responses can still be recorded over time in absence of healthy FG transport to the medulla. Using our methodology, we successfully detected varied CNAP responses in 13 of our stimulated animals prior to LPS administration and stimulation treatment. Despite this sign of nerve functionality in those animals, only two of the rats showing CNAP response showed indication of efferent FG transport, both attenuated, through the nerve. The resulting CNAPs could have strictly been the result of remaining healthy afferent fibers, or could have included remaining intact efferent fibers. We believe this to be a topic worthy of further exploration.

3.3. Hematoxylin and eosin (H&E) histology

Samples were sectioned either longitudinally to analyze the length of the nerve (figures 6(a)–(d)) or transversely across the diameter of the cuff to analyze the cross section of the nerve (figures 6(e) and (f)). Industry standard H&E staining was performed on all samples using standard protocols. We did not apply myelination specific stains to the nerve samples in this study.

Cuffed vagus nerves were histologically normal. The cuff was surrounded by fibrous connective tissue, epithelioid macrophages, and multinucleated giant cells; consistent with a granulomatous foreign body inflammatory reaction. Similar inflammatory cells were identified surrounding the epineurium (connective tissue surrounding the nerves), but not infiltrating the nerve. Such findings suggest a perineuritis, or inflammation surrounding the nerve, but not penetrating it. Such inflammation is commonly analyzed during cuff design and well documented in literature [52–54].

3.4. Cytokine measurements from blood (plasma) samples

We used plasma cytokine concentrations to analyze the effects of VNS on modulation of inflammatory cytokine levels in both chronic and acute environments. Only the pro-inflammatory cytokines interleukin (IL)-6 and TNF-α, and anti-inflammatory cytokine IL-10 were significantly elevated over time after injection of LPS, consistent with prior literature [55–57].

Due to a high level of variability in cytokine concentrations from sample to sample, and noise in the cytokine calibration curves in our raw data, we performed statistical analyses using angular transformations of proportional compositions of each cytokine compared to the overall content in the samples and utilized Cohen's h analysis for effect sizes. Samples collected at 90 min post-LPS injection demonstrated important distinctions between effects of stimulation with chronically and acutely cuffed vagus nerves (figure 7).

Pro-inflammatory TNF-α levels in acutely cuffed rats displayed higher proportions than in chronically cuffed animals, and acutely stimulated animals showed distinctly lower proportions than the acute controls ($h = 0.44$). This indicated a modulatory effect of stimulation on acutely cuffed subjects due to VNS. Chronically cuffed rats, however, showed virtually no impact on TNF-α due to stimulation.

The second pro-inflammatory cytokine, IL-6, showed much higher proportions in chronically cuffed animals at 90 min post-LPS challenge, than in their acute counterparts ($h > 0.8$). Both chronic and acute samples showed slightly lower proportions in stimulated animals versus controls, but neither were significant.

Anti-inflammatory IL-10 cytokine proportions again revealed no difference between stimulation and control groups in chronically cuffed rats. It did, however, show a small but statistically significant increase ($h = 0.22$) in proportions due to stimulation in acutely cuffed animals over the acute controls.

A decrease in TNF-α proportion and increase in IL-10 in our acutely cuffed rats were both convincing indications of inflammatory modulation using our Bionode system, consistent with similar work by multiple groups mentioned earlier presenting repeatable cytokine modulation in acute environments. Chronically cuffing the vagus nerve resulted in distinctly different cytokine proportion trends from those of our established acute baselines. Importantly, it appeared to stunt all ability to modulate plasma cytokine levels with stimulation. Having already established a critical physiological lapse in the vagus nerve's ability to transport FG in a rat when cuffed, we hypothesized, accordingly, that chronic vagal nerve cuffing also compromises the vagus nerve's ability to modulate inflammation.

3.5. Gastric emptying

Gastric functions have been shown to be primarily modulated with vagal sensory and motor signals as was investigated by Travagli *et al* [58], and alterations in those vagal signals can result in altered gastric functions [59]. Accordingly, gastric physiology such as emptying rates is a good measure to determine an altered state of vagal nerve operation. Utilizing MRI to determine gastric functions in humans has been well documented [60–62], and a similar

approach is being taken in collaborative research efforts to test gastric functions in an acute rat model [49].

To further verify our chronic cuffing hypothesis, six rats were outfitted with a single stimulation cuff on the left vagus nerve and recovered. These rats were scanned using MRI to determine stomach emptying rates first as non-stimulated controls, and a second time after a recovery and re-training period, with stimulation. Those animals that produced reliable data according to our methods were used for comparison (figure 8).

Control scans with no stimulation applied revealed a similar overall emptying effect to those that received VNS. Both groups resulted in a stomach volume reduction of ~25% from their starting volumes after 225 min. This is also in line with an acute control group that showed an average volume decrease of ~27% over the same time period [49]. While the stimulation sample size used is small due to discarded samplings, it nevertheless showed a negligible overall variation between stimulation and control. The chronic stimulation samples do show an increased emptying rate from the 30 to 90 min time points which could be a result of remaining intact efferent nerve fibers given that neither animal used for this data set showed a complete suppression of efferent FG transport. The increased rate however slows after the 90 min point. This lacking overall effect of stimulation on stomach emptying rate of chronically cuffed rats contrasted with significant and continued increases in emptying rates seen between acutely cuffed and stimulated rats in the referenced collaborative studies (not shown), and indicated a compromise of vagus nerve function likely due to chronic cuffing.

In addition, we noted a delayed emptying period, with a slight increase in stomach volume, in half of our chronic controls from the 30 to 75 min time points. This increase is also a strong indicator of an altered gastric function due to the chronic cuffing of the left vagus nerve given that it was not observed in acute controls [49].

4. Discussion

The prominent finding in our study is that chronic cuffing of the vagus nerve in a rat creates an unreliable model for VNS studies. To date, cuffing the nerve caused still unexplored physiological effects, that suppressed efferent retrograde tracer transport mechanisms, affected the vagal anti-inflammatory response to an LPS challenge, and degraded the response of gastric emptying rates to VNS. These adverse effects persisted despite a healthy outward appearance through visual and histological observation, and a full functionality of the nerve to create a CNAP response in the caudal direction from the stimulation cuff.

A shortcoming in this study was our decision not to implement a myelin specific stain such as Luxol fast blue and utilize electron microscopy to monitor potential demyelination effects that would be undetectable with basic H&E staining. It is therefore possible that while we did not observe any gross nerve alteration, local demyelination could have been present that would help explain attenuated effects of VNS in our study. Still, even observed morphological changes cannot always be linked directly to functional deficits with respect to electrical stimulation [54].

It followed that cuffing the nerve produced inflammatory foreign body response around the material of the cuff, creating a fibrotic layer of inflammatory cells between the nerve and inner cuff. Thil *et al* [53] showed that this process most commonly resulted in a stabilized interface after about 30 d, but also presented evidence that this foreign body response can penetrate into the epineurium, and that even small manipulations and deformations can cause effects in the nerve anatomy. This is supported by Tyler *et al* [63] whose flat interface nerve electrodes showed that larger manipulations of the nerve caused increased breakdowns and demyelination of nerve tissue.

Furthermore, Rydevic *et al* [64] demonstrated that applied pressures as small as 20 mmHg could introduce interference with intraneural blood flow to peripheral nerves. Theoretical pressure calculations of a split-ring cuff such as ours were presented by Naples *et al* [65] and experimentally verified by Cuoco *et al* [66]. Using their computations and accounting for a full 133% nerve swelling effect, our cuffs could be utilized on a nerve diameter greater than 600 μm (almost double the diameter of some cervical vagus nerves we measured) and not pass the 20 mmHg pressure threshold. We accordingly believe our cuffs had sufficient diameter to cuff the cervical vagus nerve in a rat safely.

Even a loosely fitting cuff though, can exert minor manipulations to the outer edges of the enclosed nerve tissue. Evidence from a study by Evans *et al* [67] suggested that motor fibers of the vagus nerve of a rabbit were commonly found grouped toward the edges of the nerve. Following this logic, it is possible that the efferent fibers in the vagus nerve of a rat would be similarly located in the lateral part of the nerve and be most susceptible to cuffing manipulations and related physiological effects. There is very little literature to support this claim in rats, however.

The possibility remains that efferent nerve fiber functionality may be severely attenuated while afferent fibers remain intact. Indeed, Phillips *et al* [42, 68], and more recently, Payne *et al* [69], reported on motor axons' inability to regenerate after nerve injury, while sensory axons did. While still speculative, our results support this hypothesis by noting the illumination of FG in the nodose ganglia of cuffed nerves while FG transport to the medulla is completely suppressed. If this is the case, studies concentrating on afferent effects of VNS may be minimally impaired by this cuffing effect. Moreover, if vagal efferent fibers are not working correctly, but afferent fibers are, VNS could negatively affect para-sympathetic systems, such as the inflammatory reflex, by sending afferent signals to the brain to increase inflammation, while suppressing the anti-inflammatory efferent signal. Suppression of the desired anti-inflammatory signal helps explain the lack of VNS effects in our study.

Concerning electrophysiological nerve functionality, the encapsulation process can take weeks or months to stabilize, making the cuff/nerve interface variable during the healing process. Sahyouni *et al* [52] explored short and long term electrical threshold changes that all eventually stabilized for stimulation purposes. Our results reflected this as the CNAP response showed to be variable during our regular four-week recovery period. Therefore, it was important to verify that a given stimulation profile was inducing a desired CNAP response before utilizing such profile to induce a biological response. A legitimate argument can be made that using a variable set of pre-stimulations, such as we did, introduced an

unknown variable into our methodology. However, a number of acute studies have used pre-stimulation as a standard procedure [8, 16–18], and an initial study was done on the potential benefits of a pre-stimulation period [13], finding it not to have a noticeable effect either way on experimental results. The topic of pre-stimulation during VNS application is worthy of further investigation in both acute and chronic settings.

No correlation, however, was found between different profiles of electrical stimulation through our cuffs with varying CNAP responses, and attenuation of FG transport in the nerve. We surmise that electrophysiological signals, while potentially affected by surgical nerve cuffing, are not alone, a conclusive indicator of potential neural damage as CNAP response can still be present in the absence of efferent FG transport.

In addition to the lack of retrograde transport integrity, we verified differences between chronically and acutely cuffed nerves in two separate measures of vagal physiological control. While noisy and variable in raw concentration levels, we nevertheless noted significant variations in plasma cytokine responses between acutely and chronically cuffed data samples when presented as percentages of an overall cytokine make-up: arguably a more robust method of analysis due to our use of a thorough 13-cytokine makeup. We discovered a complete lack of cytokine modulation through VNS when chronic cuffing was applied. Meanwhile, the influence of stimulation on gastric emptying was also revealed to be inconsequential when chronic cuffing was utilized. We did not endeavor to interpret specific physiological effects of either acute portion of these tests here, as they will be thoroughly scrutinized in separate and ongoing studies for future publication. Our primary finding was an established disparity between acutely and chronically cuffed vagus nerves, and evidence of compromised vagus nerve functionality when chronically cuffed.

An analysis of notable distinctions in the reviewed chronic VNS literature allows us to discuss potential pros and cons of prior studies. Nearly half of the reviewed studies utilized industry-made helical electrodes (Cyberonics). This helical design has shown to be mechanically advantageous in reducing mechanical stresses directly to the nerve in human subjects [70]. In rat subjects, the implantation involved wrapping the electrodes around the entire carotid sheath rather than the nerve being dissected away from the carotid artery before being independently cuffed [15, 22–24, 31, 33]. Anchoring to the artery conceivably allowed more support for the cuff and significantly reduced the mechanical manipulation to the nerve itself, but also likely resulted in less surface contact of the electrode with the nerve and, expectedly, a less-focused stimulation to the nerve. It is unlikely that such an arrangement would be sufficient for studies wishing to selectively stimulate specific fiber types and accurately record CNAP responses in a closed-loop arrangement. It would be pertinent to explore the effect this cuffing strategy might have on retrograde tracer transport.

A second noteworthy difference in reviewed publications was in the method and length of stimulation employed. Most studies utilized a chronic stimulation strategy that stimulated the nerve for continuous stretches throughout days, weeks, and even months which is inconsistent with our singular 5 min stimulation in response to an acute LPS injection. It is possible that effects of chronic stimulation can overcome inhibition of vagal efferent fibers over the course of time with repeated application, working through separate secondary para-

sympathetic pathways. It is also feasible that over the course of time parts of the nerve interface did heal and allow some function of the vagal efferent fibers [69, 71, 72]. This, however, is not supported by our results that showed no improvement of FG transport over 13–71 d recovery periods.

In summary, despite the body of previously performed studies utilizing chronic nerve cuffing for VNS trials, we believe we are the first to employ our novel combination of integrity checks of the nerve. To our knowledge, there was only one previous chronic VNS study that centered on inflammatory effects in the gastric region of rats [33]. While their results are compelling, the significance of cytokine modulation they reported is in contrast with our findings. Variations in cuff designs, surgical techniques, or stimulation strategies they utilized could account for this, but without further study on the integrity of nerves prepared with theirs' and others' methods, we can only speculate. We have, however, presented evidence of physiological degradation of vagus nerve functionality when utilizing our methods of chronic cuffing for VNS therapy in rats in the form of suppressed efferent FG transport, and altered effects on inflammatory cytokine modulation and gastric emptying. To confidently and reliably continue advancement in the science of chronic VNS, such effects should be seriously considered and further investigated by the VNS community as a whole.

Supplementary Material

Refer to Web version on PubMed Central for supplementary material.

Acknowledgments

Expressed thanks to Bartek Rajwa of Purdue's Bindley Bioscience Center for his statistics expertise, Jennifer Sturgis and Kathy Ragheb of the Purdue Cytometry Laboratories, Dr Robert Phillips, Elizabeth Baronowsky, Jennifer McAdams and Diana Black of the Purdue Department of Psychological Sciences, Steven Oleson of the Purdue Laboratory of Integrated Brain Imaging, Robyn McCain of the Purdue Translational Pharmacology Unit, Victor Bernal-Crespo of the Purdue Veterinary School Histology Laboratory, and Quan Yuan, Mark Bevilacqua, Shelby Olson, Grant Wang, Jui-Wei Tsai, and Emily Martin of the Purdue Center for Implantable Devices.

Research supported by the Defense Advanced Research Projects Agency (DARPA) ElectRx program under the auspices of Dr Douglas Weber, Grant No. N66001-15-2-4056. Any opinion, findings, and conclusions or recommendations expressed in this material are those of the authors(s) and do not necessarily reflect the views of DARPA.

References

[1]. Grimonprez A, Raedt R, Baeken C, Boon P and Vonck K 2015 The antidepressant mechanism of action of vagus nerve stimulation: evidence from preclinical studies Neurosci. Biobehav. Rev. 56 26–34 [PubMed: 26116875]

[2]. Koopman F A et al. 2016 Vagus nerve stimulation inhibits cytokine production and attenuates disease severity in rheumatoid arthritis Proc. Natl Acad. Sci. USA 113 8284–9 [PubMed: 27382171]

[3]. George M S M, Nahas Z M, Bohning D E P, Kozel F A M, Anderson B R, Chae J H M, Lomarev MMDP, Denslow SP, Li XM and Mu CMDP 2002 Vagus nerve stimulation therapy: a research update Neurology 59 S56–61 [PubMed: 12270970]

[4]. Groves D A and Brown V J 2005 Vagal nerve stimulation: a review of its applications and potential mechanisms that mediate its clinical effects Neurosci. Biobehav. Rev. 29 493–500 [PubMed: 15820552]

[5]. Panescu D 2005 Vagus nerve stimulation for the treatment of depression IEEE Eng. Med. Biol. Mag. 24 68–72

[6]. Tracey K 2002 The inflammatory reflex Nature 420 853–9 [PubMed: 12490958]

[7]. Pavlov V A, Wang H, Czura C J, Friedman S G and Tracey K J 2003 The cholinergic anti-inflammatory pathway: a missing link in neuroimmunomodulation Mol. Med. 9 125 [PubMed: 14571320]

[8]. Rosas-Ballina M, Ochani M, Parrish W R, Ochani K, Harris Y T, Huston J M, Chavan S and Tracey K J 2008 Splenic nerve is required for cholinergic antiinflammatory pathway control of TNF in endotoxemia Proc. Natl Acad. Sci. USA 105 11008 [PubMed: 18669662]

[9]. Rosas-Ballina M et al. 2011 Acetylcholine- synthesizing T cells relay neural signals in a vagus nerve circuit Science 334 98–101 [PubMed: 21921156]

[10]. Andersson U and Tracey K J 2012 Neural reflexes in inflammation and immunity J. Exp. Med. 209 1057–68 [PubMed: 22665702]

[11]. Martelli D, McKinley M J and McAllen R M 2014 The cholinergic anti-inflammatory pathway: a critical review Auton. Neurosci. 182 65–9 [PubMed: 24411268]

[12]. Bonaz B, Sinniger V and Pellissier S 2016 Anti-inflammatory properties of the vagus nerve: potential therapeutic implications of vagus nerve stimulation J. Physiol. 594 5781–90 [PubMed: 27059884]

[13]. Patel Y A, Saxena T, Bellamkonda R V and Butera R J 2017 Kilohertz frequency nerve block enhances anti-inflammatory effects of vagus nerve stimulation Sci. Rep. 7 39810 [PubMed: 28054557]

[14]. Clark K B, Smith D C, Hassert D L, Browning R A, Naritoku D K and Jensen R A 1998 Posttraining electrical stimulation of vagal afferents with concomitant vagal efferent inactivation enhances memory storage processes in the rat Neurobiol. Learn. Mem. 70 364–73 [PubMed: 9774527]

[15]. Cunningham J T, Mifflin S W, Gould G G and Frazer A 2008 Induction of c-Fos and DeltaFosB immunoreactivity in rat brain by vagal nerve stimulation Neuropsychopharmacology 33 1884–95 [PubMed: 17957222]

[16]. Borovikova L V 2000 Vagus nerve stimulation attenuates the systemic inflammatory response to endotoxin Nature 405 458–63 [PubMed: 10839541]

[17]. Huston J M, Ochani M, Rosas-Ballina M, Liao H, Ochani K, Pavlov V A, Gallowitsch-Puerta M, Ashok M, Czura C J and Foxwell B 2006 Splenectomy inactivates the cholinergic antiinflammatory pathway during lethal endotoxemia and polymicrobial sepsis J. Exp. Med. 203 1623–8 [PubMed: 16785311]

[18]. Bernik T R, Friedman S G, Ochani M, DiRaimo R, Ulloa L, Yang H, Sudan S, Czura C J, Ivanova S M and Tracey K J 2002 Pharmacological stimulation of the cholinergic antiinflammatory pathway J. Exp. Med. 195 781–8 [PubMed: 11901203]

[19]. Sanders R D, Hussell T and Maze M 2009 Sedation and immunomodulation Crit. Care Clin 25 551–70 [PubMed: 19576530]

[20]. Picq C A, Clarençon D, Sinniger V E, Bonaz B L and Mayol J-F S 2013 Impact of anesthetics on immune functions in a rat model of vagus nerve stimulation PLoS One 8 e67086 [PubMed: 23840592]

[21]. Krahl S E, Senanayake S S and Handforth A 2001 Destruction of peripheral C-fibers does not alter subsequent vagus nerve stimulation-induced seizure suppression in rats Epilepsia 42 586

[22]. Dorr A E and Debonnel G 2006 Effect of vagus nerve stimulation on serotonergic and noradrenergic transmission J. Pharmacol. Exp. Ther. 318 890–8 [PubMed: 16690723]

[23]. Handforth A and Krahl S E 2001 Suppression of harmalineinduced tremor in rats by vagus nerve stimulation Mov. Disorders 16 84–8

[24]. Biggio F, Gorini G, Utzeri C, Olla P, Marrosu F, Mocchetti I and Follesa P 2009 Chronic vagus nerve stimulation induces neuronal plasticity in the rat hippocampus Int. J. Neuropsychopharmacol 12 1209–21 [PubMed: 19309534]

[25]. Chunchai T, Samniang B, Sripetchwandee J, Pintana H, Pongkan W, Kumfu S, Shinlapawittayatorn K,KenKnight B H, Chattipakorn N and Chattipakorn S C 2016 Vagus nerve

stimulation exerts the neuroprotective effects in obese-insulin resistant rats, leading to the improvement of cognitive function Sci. Rep. 6 26866 [PubMed: 27226157]

[26]. Grimonprez A, Raedt R, Dauwe I, Mollet L, Larsen L E, Meurs A, De Herdt V, Wadman W, Delbeke J and Vonck K 2015 Vagus nerve stimulation has antidepressant effects in the kainic acid model for temporal lobe epilepsy Brain Stimul. 8 13–20 [PubMed: 25444592]

[27]. Zhang X, Cao B, Yan N, Liu J, Wang J, Tung V O V and Li Y 2013 Vagus nerve stimulation modulates visceral painrelated affective memory Behav. Brain Res. 236 8–15 [PubMed: 22940455]

[28]. Peña D F, Childs J E, Willett S, Vital A, McIntyre C K and Kroener S 2014 Vagus nerve stimulation enhances extinction of conditioned fear and modulates plasticity in the pathway from the ventromedial prefrontal cortex to the amygdala Frontiers Behav. Neurosci 8 327

[29]. Agarwal R, Mokelke E, Ruble S B and Stolen C M 2016 Vagal nerve stimulation evoked heart rate changes and protection from cardiac remodeling J. Cardiovasc. Transl. Res. 9 67–76 [PubMed: 26746408]

[30]. Chapleau M W, Rotella D L, Reho J J, Rahmouni K and Stauss H M 2016 Chronic vagal nerve stimulation prevents high-salt diet-induced endothelial dysfunction and aortic stiffening in stroke-prone spontaneously hypertensive rats Am. J. Physiol. Heart. Circ. Physiol 311 H276–85 [PubMed: 27208157]

[31]. Lee S W, Li Q, Libbus I, Xie X, KenKnight B H, Garry M G and Tolkacheva E G 2016 Chronic cyclic vagus nerve stimulation has beneficial electrophysiological effects on healthy hearts in the absence of autonomic imbalance Physiol. Rep. 4 e12786 [PubMed: 27173672]

[32]. Zheng C, Li M, Kawada T, Uemura K, Inagaki M and Sugimachi M 2014 A practical use method of chronic vagal stimulation in rats Biomed. Eng 52 O-438–9

[33]. Meregnani J et al. 2011 Anti-inflammatory effect of vagus nerve stimulation in a rat model of inflammatory bowel disease Auton. Neurosci 160 82–9 [PubMed: 21071287]

[34]. El Tahry R et al. 2011 Repeated assessment of larynx compound muscle action potentials using a self-sizing cuff electrode around the vagus nerve in experimental rats J. Neurosci. Methods 198 287–93 [PubMed: 21513735]

[35]. Loeb G E. 1996; Cuff electrodes for chronic stimulation and recording of peripheral nerve activity. J. Neurosci. Methods. 64:95. [PubMed: 8869489]

[36]. Rodri F J, Ceballos D, Schu M, Valero A, Valderrama E, Stieglitz T and Navarro X 2000 Polyimide cuff electrodes for peripheral nerve stimulation J. Neurosci. Methods 98 105–18 [PubMed: 10880824]

[37]. Lee Y J, Kim H J, Kang J Y, Do S H and Lee S H 2017 Biofunctionalization of nerve interface via biocompatible polymer-roughened Pt black on cuff electrode for chronic recording Adv. Healthcare Mater. 6 1601022

[38]. Ware T, Simon D, Rennaker R L and Voit W 2013 Smart polymers for neural interfaces Polym. Rev 53 108–29

[39]. Pederson D J, Quinkert C J, Arafat M A, Somann JP, Williams J D, Bercich R A, Wang Z, Albors G O, Jefferys J G R and Irazoqui P P 2017 The design of the bionode: an implantable wireless electroceutical device for recording and stimulating bioelectric events IEEE Trans. Biomed. Eng 64 775–85 [PubMed: 27295647]

[40]. Powley T L, Fox E A and Berthoud H R 1987 Retrograde tracer technique for assessment of selective and total subdiaphragmatic vagotomies Am. J. Physiol 253 R361–70 [PubMed: 3618835]

[41]. Phillips R J and Powley T L 1998 Gastric volume detection after selective vagotomies in rats Am. J. Physiol 274 R1626–38 [PubMed: 9608017]

[42]. Phillips R J, Baronowsky E A and Powley T L 2000 Regenerating vagal afferents reinnervate gastrointestinal tract smooth muscle of the rat J. Comp. Neurol. 421 325–46 [PubMed: 10813790]

[43]. Bioanalytical Systems I 2007 Surgical procedures: femoral cannulation (rat) Surgery Manual Culex ABS (West Lafayette, IN: Bioanalytical Systems Inc.)

[44]. Peters S, Hampsch J, Cregor M, Starrett C, Gunaratna G and Kissinger C 2000 Culex ABS part I: introduction to automated blood sampling Curr. Separations 18 140

[45]. Bohs C, Cregor M, Gunaratna G and Kissinger C 2000 Culex automated blood sampler part II: managing freely-moving animals and monitoring their activity Curr. Separations 18 148

[46]. Ward M P, Qing K Y, Otto K J, Worth R M, John S W M and Irazoqui P P 2015 A flexible platform for biofeedback- driven control and personalization of electrical nerve stimulation therapy IEEE Trans. Neural Syst. Rehabil. Eng. 23 475–84 [PubMed: 25167554]

[47]. Ward M P and Nowak T V 2017 A new approach to study vagal control of stomach function 2017 Annual Meeting of the Biomedical Engineering Society (Phoenix, AZ)

[48]. Fogel R, Zhang X and Renehan W E 1996 Relationships between the morphology and function of gastric and intestinal distention-sensitive neurons in the dorsal motor nucleus of the vagus J. Comp. Neurol 364 78–91 [PubMed: 8789277]

[49]. Lu K H, Cao J, Oleson S, Powley T L and Liu Z 2017 Contrast enhanced magnetic resonance imaging of gastric emptying and motility in rats IEEE Trans. Biomed. Eng. 64 2546–54 [PubMed: 28796602]

[50]. Zaaimi B, Grebe R and Wallois F 2008 Animal model of the short-term cardiorespiratory effects of intermittent vagus nerve stimulation Auton. Neurosci 143 20–6 [PubMed: 18757249]

[51]. Mermelstein M, Nonweiler R and Rubinstein E H 1996 Intraoperative identification of laryngeal nerves with laryngeal electromyography Laryngoscope 106 752–6 [PubMed: 8656962]

[52]. Sahyouni R, Chang D T, Moshtaghi O, Mahmoodi A, Djalilian H R and Lin H W 2017 Functional and histological effects of chronic neural electrode implantation Laryngosc. Invest. Otolaryngol 2 80–93

[53]. Thil M A, Duy D T, Colin I M and Delbeke J 2007 Time course of tissue remodelling and electrophysiology in the rat sciatic nerve after spiral cuff electrode implantation J. Neuroimmunol 185 103–14 [PubMed: 17343923]

[54]. Grill W M and Mortimer J T 2000 Neural and connective tissue response to long-term implantation of multiple contact nerve cuff electrodes J. Biomed. Mater. Res A 50 215–26

[55]. Flohe S, Fernandez E D, Ackermann M, Hirsch T, Börgermann J and Schade F 1999 Endotoxin tolerance in rats: expression of TNF-α, IL-6, IL-10, VCAM-1 and HSP70 in lung and liver during endotoxin shock Cytokine 11 796–804 [PubMed: 10525319]

[56]. Waage A 1987 Production and clearance of tumor necrosis factor in rats exposed to endotoxin and dexamethasone Clin. Immunol. Immunopathol 45 348–55 [PubMed: 3315338]

[57]. Kakizaki Y, Watanobe H, Kohsaka A and Suda T 1999 Temporal profiles of interleukin-1β, Interleukin-6, and tumor necrosis factor-α in the plasma and hypothalamic paraven-tricular nucleus after intravenous or intraperitoneal administration of lipopolysaccharide in the rat Endocrine J. 46 487–96 [PubMed: 10580740]

[58]. Travagli R A and Anselmi L 2016 Vagal neurocircuitry and its influence on gastric motility Nat. Rev. Gastroenterol. Hepatol 13 389–401 [PubMed: 27251213]

[59]. McMenamin C A, Travagli R A and Browning K N 2016 Inhibitory neurotransmission regulates vagal efferent activity and gastric motility Exp. Biol. Med. 241 1343–50

[60]. Schwizer W, Steingoetter A and Fox M 2006 Magnetic resonance imaging for the assessment of gastrointestinal function Scand. J. Gastroenterol 41 1245–60 [PubMed: 17060117]

[61]. Marciani L 2011 Assessment of gastrointestinal motor functions by MRI: a comprehensive review Neurogastroenterol. Motility 23 399–407

[62]. de Zwart I M and de Roos A 2010 MRI for the evaluation of gastric physiology Eur. Radiol. 20 2609–16 [PubMed: 20585784]

[63]. Tyler D J and Durand D M 2003 Chronic response of the rat sciatic nerve to the flat interface nerve electrode Ann. Biomed. Eng 31 633–42 [PubMed: 12797612]

[64]. Rydevik B, Lundborg G and Bagge U 1981 Effects of graded compression on intraneural blood flow: an in vivo study on rabbit tibial nerve J. Hand Surg 6 3–12

[65]. Naples G G 1988 A spiral nerve cuff electrode for peripheral nerve stimulation IEEE Trans. Biomed. Eng. 35 905 [PubMed: 3198136]

[66]. Cuoco F A Jr 2000 Measurement of external pressures generated by nerve cuff electrodes IEEE Trans. Rehabil. Eng. 8 35 [PubMed: 10779106]

[67]. Evans D and Murray J 1954 Histological and functional studies on the fibre composition of the vagus nerve of the rabbit J. Anat. 88 320–37 [PubMed: 13192020]

[68]. Phillips R J, Baronowsky E A and Powley T L 2003 Longterm regeneration of abdominal vagus: efferents fail while afferents succeed J. Comp. Neurol 455 222–37 [PubMed: 12454987]

[69]. Payne S C, Belleville P J and Keast J R 2015 Regeneration of sensory but not motor axons following visceral nerve injury Exp. Neurol 266 127–42 [PubMed: 25725351]

[70]. Navarro X 2005 A critical review of interfaces with the peripheral nervous system for the control of neuroprostheses and hybrid bionic systems J. Peripher. Nervous Syst. 10 229–59

[71]. Guth L and Jacobson S 1966 The rate of regeneration of the vagus nerve of the cat Exp. Neurol 14 439–47 [PubMed: 4378198]

[72]. Kanje M 1991 Survival and regeneration of the adult rat vagus nerve in culture Brain Res. 550 340–2 [PubMed: 1715807]

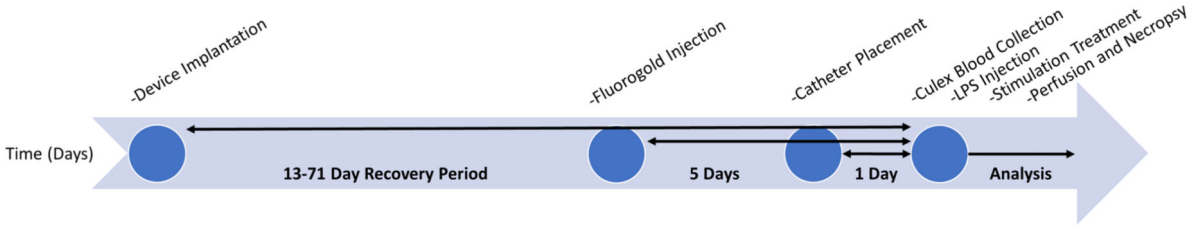

Figure 1.

Time flow diagram of our chronic experimental design. Chart outlines the overall long-term flow of our experiment over the course of weeks, beginning with surgical implantation and flowing though data analysis.

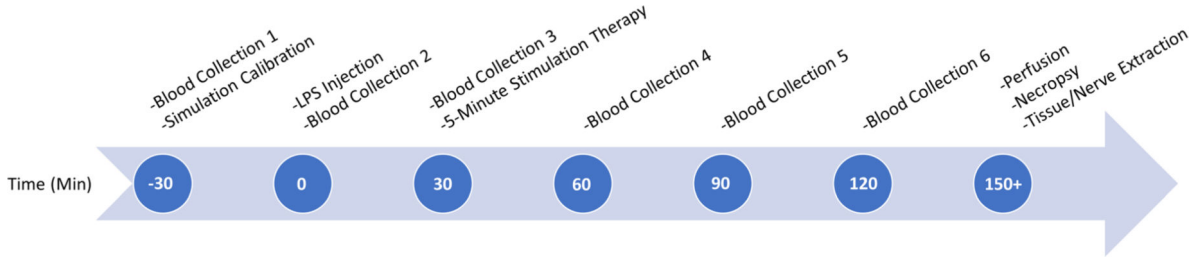

Figure 2.

Time flow diagram outlines the process of blood collection on the last day of chronic experiments. Time points are based with relation to the acute LPS injection of the animal.

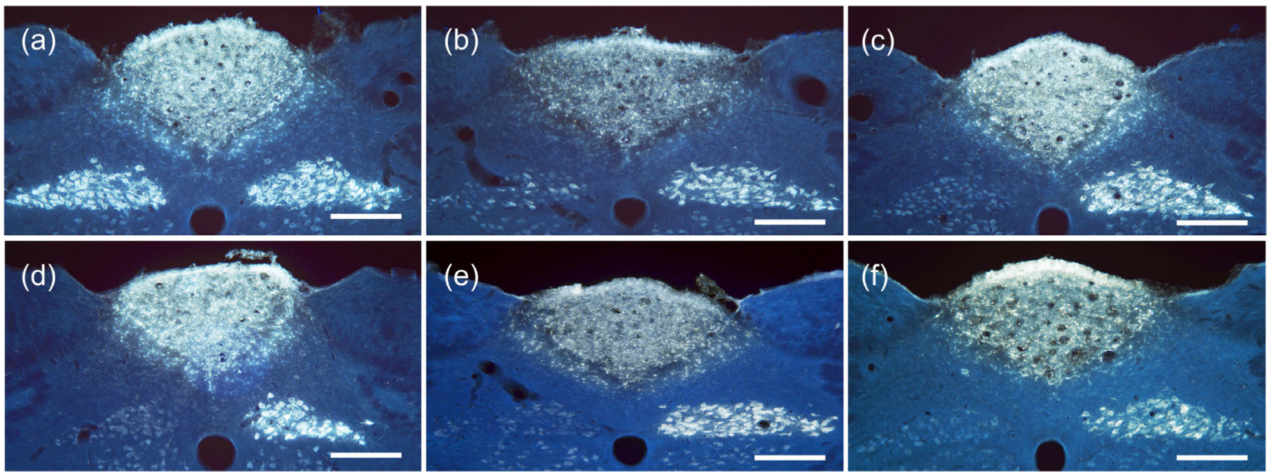

Figure 3.

Fluorescent images of medulla samples from multiple cuffing variations of rats. (a) Cuffs placed adjacent to left vagus nerve, but not enclosing it (eRx110), produced bright efferent fiber FG transport illumination on both left and right sides of DMN. (b) Cuffed with standard record and stimulation cuffs by visiting surgeon (eRx116), showing bright FG illumination on the right side of the DNM from uncuffed right vagus nerve, but limited efferent transport from the left vagus on the left side of the DMN. (c)–(f) All rat medulla samples showed near-complete suppression of efferent transport on the left side. (c) Cuffed with single industry-made (CorTec; Freiburg, Germany) tunnel electrode with 0.6 mm inner diameter (eRx118). (d) Cuffed with a single standard stimulation cuff (eRx113). (e) Cuffed with sham record and stimulation cuffs containing no metal electrodes (eRx132). (f) Cuffed with standard record and stimulation cuffs, but not stimulated (eRx75). Scale bars = 250 microns.

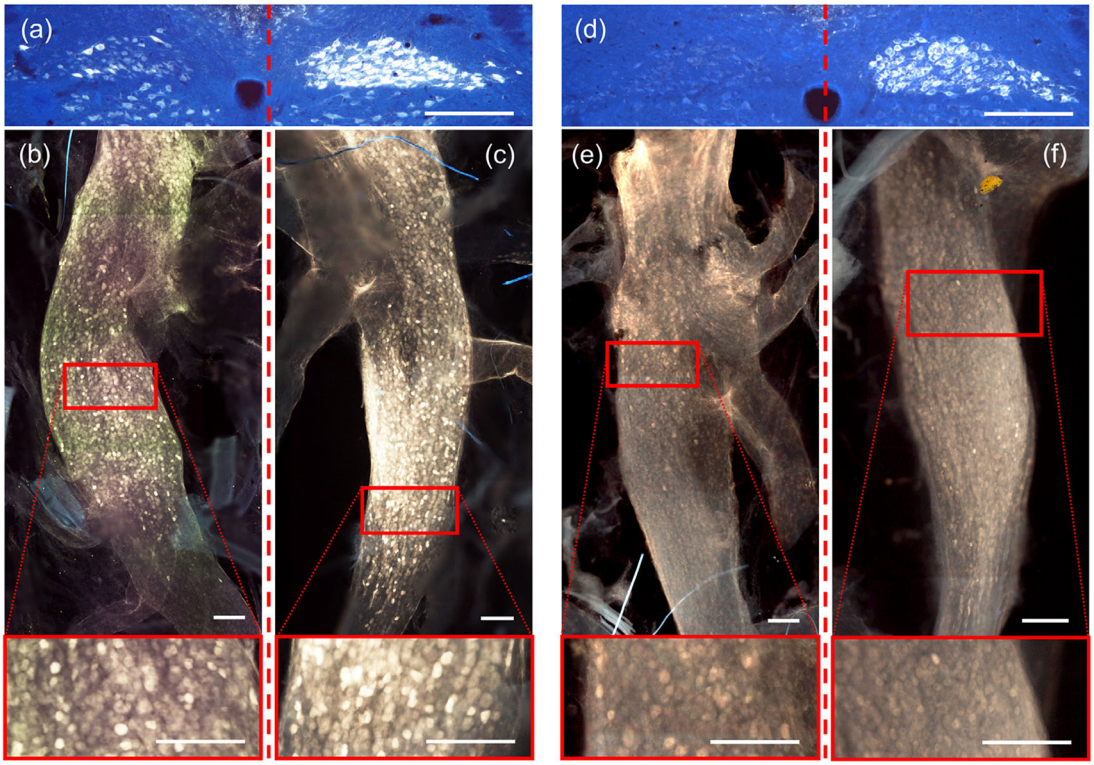

Figure 4.

Comparative fluorescence images of two separate rats demonstrating healthy FG transport through efferent fibers to the DMN and afferent fibers to the nodose in uncuffed right vagus nerves, but only through afferent fibers in cuffed left vagus nerves. (a) medulla image (from eRx159) showing clear efferent fiber FG illumination on the right side of the DMN, and severe suppression of FG on the left side. (b) and (c) corresponding fluorescence nodose images of the cuffed left and uncuffed right (respectively) vagus nerves (from eRx159), with enhanced images (red boxes) highlighting FG illuminated cells on both sides. (d) medulla image (from eRx163) also showing strong efferent fiber FG illumination on the right side of the DMN, and complete suppression of FG on the left side. (e) and (f) Corresponding fluorescence nodose images of the cuffed left and uncuffed right (respectively) vagus nerves (from eRx163), with enhanced images highlighting FG illuminated cells on both sides. Red dashed lines separate the left vagal effects from right vagal effects. Scale bars = 250 microns.

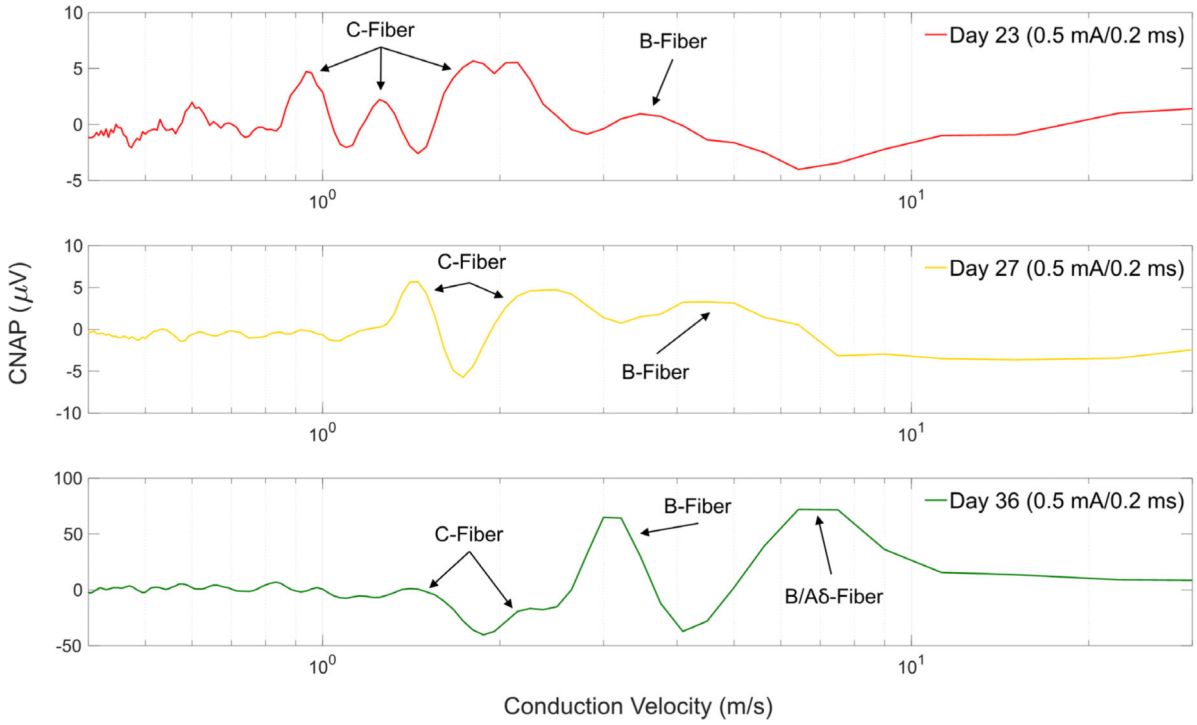

Figure 5.

Representative CNAP responses of the left cervical vagus nerve in a rat subject (eRx144) show variance in fiber responses to similar stimulation over multiple days after three weeks of recovery. Similar CNAP responses were seen in multiple animals despite having suppressed FG transport. Fiber labels were calculated using conduction velocities based on measured distance between stimulation and recording cuff at time of chronic implantation. No measurements were made during necropsy to verify original cuff distances.

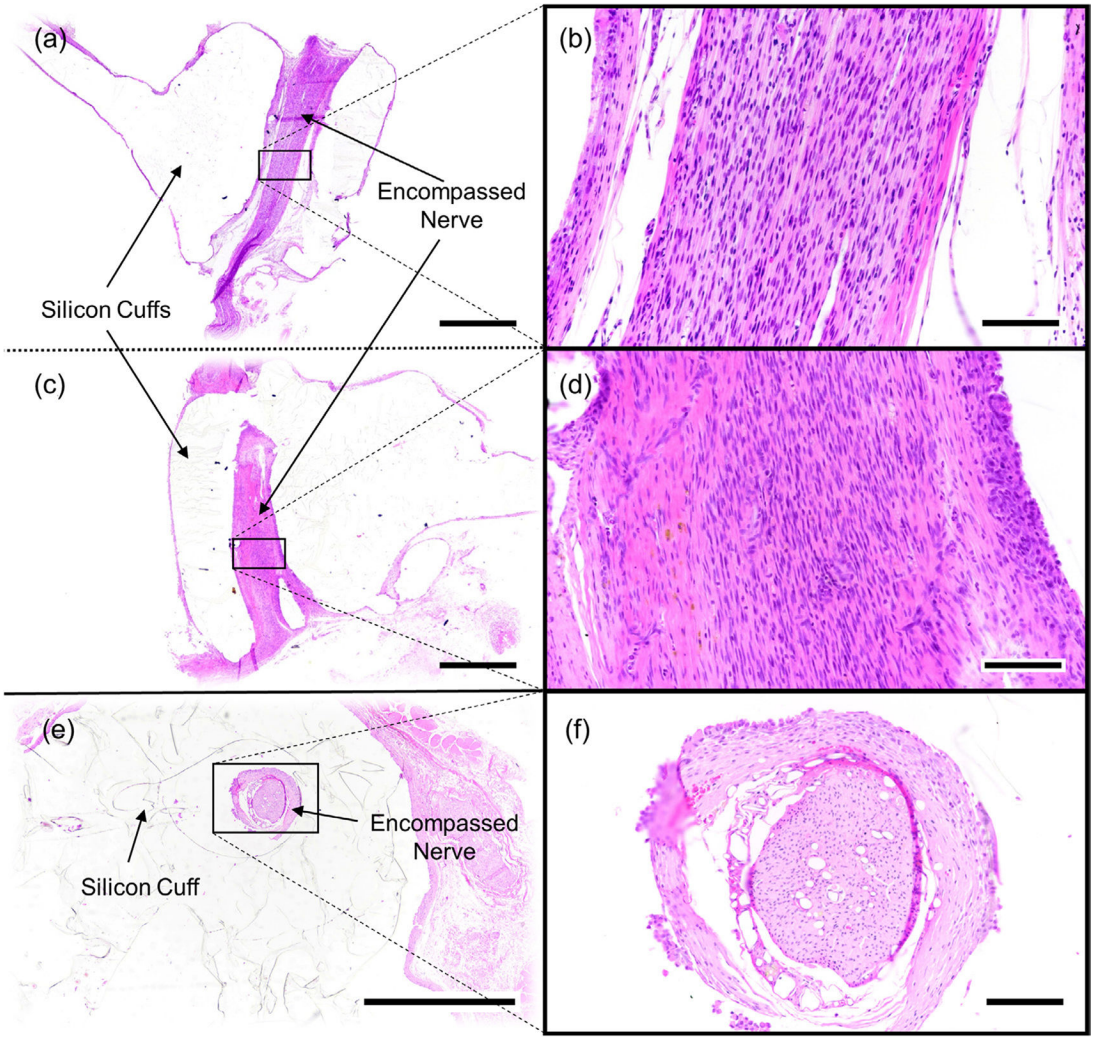

Figure 6.

Representative photomicrographs of cuffed vagus nerves stained with hematoxylin and eosin (HE). Images ((a)–(d)) are from the same nerve (eRx143). Images ((e) and (f)) are of a separate nerve (eRx132). (a) Longitudinally sectioned nerve encompassed by a stimulation cuff, (b) higher magnification of (a). (c) Longitudinally sectioned nerve encompassed by a caudally positioned recording cuff, (d) higher magnification of (c). (e) Example of a nerve cuffed with an inert cuff with no metal electrodes sectioned in the transverse plane, (f) higher magnification of (e). Scale bars = 1000 microns ((a), (c) and (e)) or 100 microns ((b), (d) and (f)).

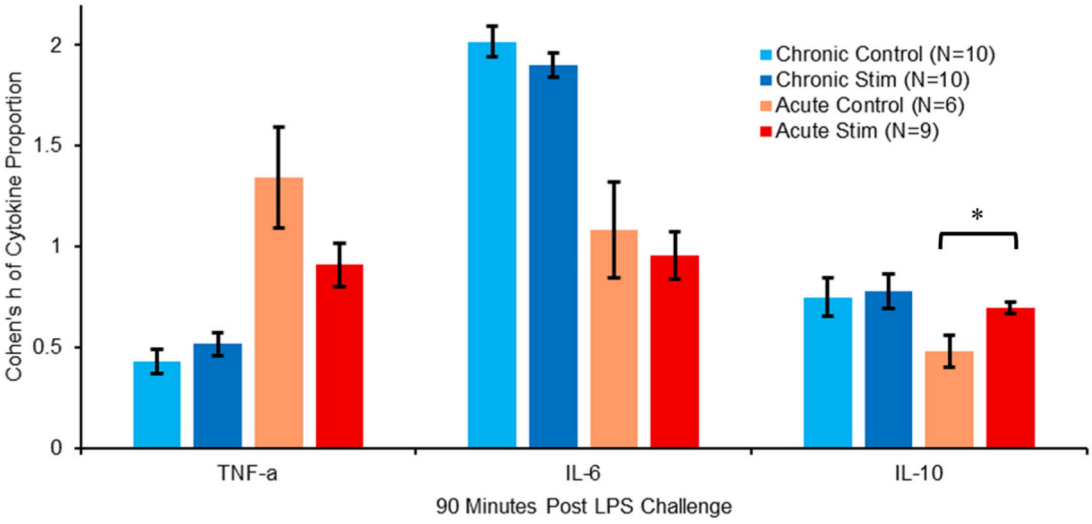

Figure 7.

Plot shows compositional analysis with angular (arcsin) transformations of proportional make-up in specific cytokine levels at 90 min post-LPS injection. Acute subjects showed a decrease in TNF-α proportion ($h > 0.4$) and a small ($h < 0.25$) but significant increase in IL-10 proportion due to stimulation, indicating strong inflammatory modulation due to stimulation. Chronic subjects showed no significant modulation in proportion levels due to stimulation in any of the three cytokines, consistent with compromised vagus function after chronic cervical cuffing. Error bars, s.e.m. $*P < 0.05$.

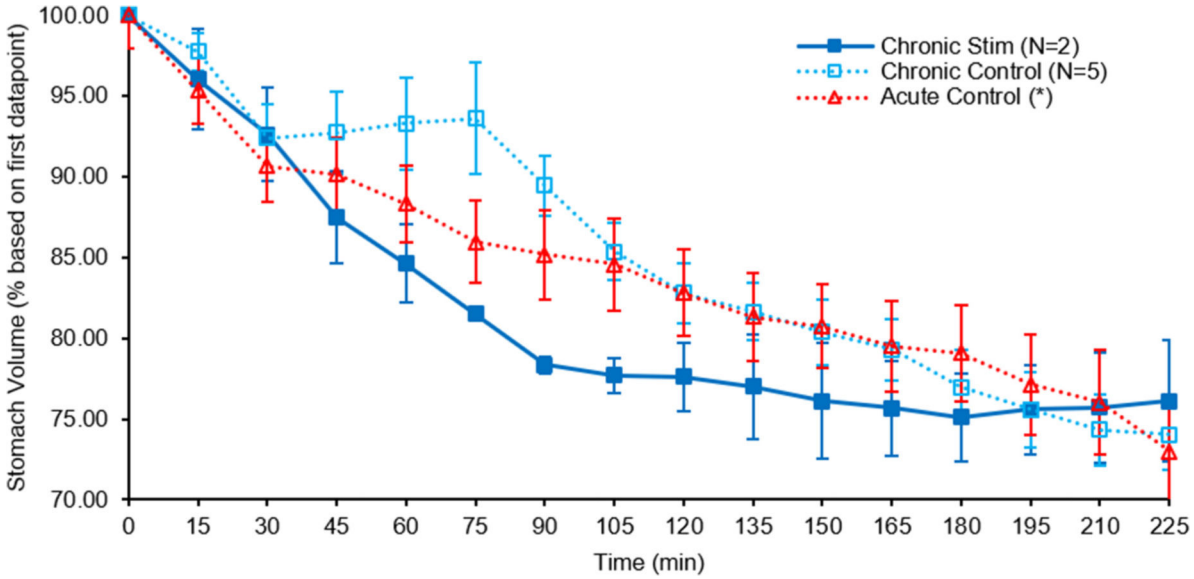

Figure 8.

Gastric (stomach) emptying rates of rats with chronically implanted vagus cuff electrodes versus acute controls. Overall emptying with stimulation in a chronically implanted animal (solid line) is indistinguishable from control (dashed line) after 4 h, unlike acute stimulation (publication in preparation), consistent with compromised vagus function after chronic cervical cuffing. *Acute control set comes from previous publication [49]. Error bars, s.e.m.